



Swansea University
Prifysgol Abertawe



Cronfa - Swansea University Open Access Repository

This is an author produced version of a paper published in :
Applied Mathematical Modelling

Cronfa URL for this paper:
<http://cronfa.swan.ac.uk/Record/cronfa32636>

Paper:

Chakraborty, S., Chatterjee, T., Chowdhury, R. & Adhikari, S. (2017). A Surrogate Based Multi-fidelity Approach for Robust Design Optimization. *Applied Mathematical Modelling*
<http://dx.doi.org/10.1016/j.apm.2017.03.040>

This article is brought to you by Swansea University. Any person downloading material is agreeing to abide by the terms of the repository licence. Authors are personally responsible for adhering to publisher restrictions or conditions. When uploading content they are required to comply with their publisher agreement and the SHERPA RoMEO database to judge whether or not it is copyright safe to add this version of the paper to this repository.
<http://www.swansea.ac.uk/iss/researchsupport/cronfa-support/>

Accepted Manuscript

A Surrogate Based Multi-fidelity Approach for Robust Design Optimization

Souvik Chakraborty, Tanmoy Chatterjee, Rajib Chowdhury,
Sondipon Adhikari

PII: S0307-904X(17)30189-0
DOI: [10.1016/j.apm.2017.03.040](https://doi.org/10.1016/j.apm.2017.03.040)
Reference: APM 11681

To appear in: *Applied Mathematical Modelling*

Received date: 2 March 2016
Revised date: 26 December 2016
Accepted date: 20 March 2017

Please cite this article as: Souvik Chakraborty, Tanmoy Chatterjee, Rajib Chowdhury, Sondipon Adhikari, A Surrogate Based Multi-fidelity Approach for Robust Design Optimization, *Applied Mathematical Modelling* (2017), doi: [10.1016/j.apm.2017.03.040](https://doi.org/10.1016/j.apm.2017.03.040)



This is a PDF file of an unedited manuscript that has been accepted for publication. As a service to our customers we are providing this early version of the manuscript. The manuscript will undergo copyediting, typesetting, and review of the resulting proof before it is published in its final form. Please note that during the production process errors may be discovered which could affect the content, and all legal disclaimers that apply to the journal pertain.

Highlights

- A surrogate based multi-fidelity framework for RDO is proposed.
- The first approach is highly efficient and requires very few actual simulations.
- Second approach yields highly accurate result from slightly increased simulation.

ACCEPTED MANUSCRIPT

A Surrogate Based Multi-fidelity Approach for Robust Design Optimization

Souvik Chakraborty^a, Tanmoy Chatterjee^a, Rajib Chowdhury^a, Sondipon Adhikari^b

^aDepartment of Civil Engineering, Indian Institute of Technology Roorkee, Roorkee, India

^bCollege of Engineering, Swansea University, Singleton Park, Swansea SA2 8PP, United Kingdom

Abstract

Robust design optimization (RDO) is a field of optimization in which certain measure of robustness is sought against uncertainty. Unlike conventional optimization, the number of function evaluations in RDO is significantly more which often renders it time consuming and computationally cumbersome. This paper presents two new methods for solving the RDO problems. The proposed methods couple differential evolution algorithm (DEA) with polynomial correlated function expansion (PCFE). While DEA is utilized for solving the optimization problem, PCFE is utilized for calculating the statistical moments. Three examples have been presented to illustrate the performance of the proposed approaches. Results obtained indicate that the proposed approaches provide accurate and computationally efficient estimates of the RDO problems. Moreover, the proposed approaches outperforms popular RDO techniques such as tensor product quadrature, Taylor's series and Kriging. Finally, the proposed approaches have been utilized for robust hydroelectric flow optimization, demonstrating its capability in solving large scale problems.

Keywords: robust design optimization, polynomial correlated function expansion, differential evolution algorithm, stochastic computation

1. Introduction

Design, construction and maintenance of engineering systems involve decision making at the managerial as well as technological level. The two primary goals of such decision are to minimize the effort required and to maximize the desired profit. In order to achieve the

Email addresses: csouvik41@gmail.com (Souvik Chakraborty), tanmoydce88@gmail.com (Tanmoy Chatterjee), rajibfce@iitr.ac.in (Rajib Chowdhury), s.adhikari@swansea.ac.uk (Sondipon Adhikari)

5 goals, techniques capable of finding the designs which meet the requirements specified by
 6 goal functions or objective functions, are needed. This process of finding the appropriate
 7 design parameters is termed as optimization. Apart from the objective function, a typical
 8 optimization also have to account for the design constraints imposed on the design variables.
 9 Such constraints are modelled by inequalities and/or equalities restricting the design space.
 10 Mathematically, an optimization problem can be stated as

$$\begin{aligned}
 & \arg \min_{\mathbf{x} \in \mathbb{R}} y_0(\mathbf{d}) \\
 & \text{s.t.} \quad y_l(\mathbf{d}) \leq 0, \quad l = 1, 2, \dots, n_c \\
 & \quad \quad d_{k,L} \leq d_k \leq d_{k,U}, \quad k = 1, \dots, n_v
 \end{aligned} \tag{1}$$

11 where \mathbf{d} denotes the design variables, $y_0 : \mathbb{R} \rightarrow \mathbb{R}^M$ denotes the objective function and $y_l :$
 12 $\mathbb{R} \rightarrow \mathbb{R}^M$, $l = 1, \dots, n_c$, $1 \leq n_c < \infty$ denotes the constraints. $d_{k,L}$ and $d_{k,U}$ are, respectively,
 13 the lower and upper bounds of the k^{th} design variable. However, Eq. (1) optimized in the
 14 classical sense is often very sensitive to small changes in design variables and may yield
 15 erroneous result due to the presence of significant uncertainties in the geometric and material
 16 properties, such as elastic modulus, cross-sectional area, density, residual strength etc. In
 17 order to overcome this issue, [1] introduced the concept of robust design optimization (RDO).
 18 RDO establishes a mathematical framework for optimization in which certain measure of
 19 robustness is sought against uncertainty. The primary aim of RDO is to minimize the
 20 propagation of uncertainties from input to output variables and thus results in an insensitive
 21 design. Over the last decade, RDO has gained vast popularity in the field of aerospace
 22 engineering [2], automotive engineering [3] marine engineering [4] and civil engineering [5, 6].
 23 The objective and/or constraints in a RDO often involve determination of the first two
 24 statistical moments of responses. Therefore, solution of a RDO problem necessitates un-
 25 certainty quantification of the response and its coupling with an optimization algorithm.
 26 Consequently, RDO demands a greater computational effort as compared to conventional
 27 optimization. The concern regarding accuracy and efficiency of existing RDO techniques is
 28 mainly two-fold.

- 29 • Firstly, most of the methods for RDO utilizes gradient based optimization (GBO).
 30 Although easy to implement, GBO often yields local optima. Alternatively, if explicit

31 functional form for objective function is not available, the gradient of objective function
32 is calculated by employing finite difference method. This renders the optimization
33 process computationally expensive.

- 34 • Secondly, the popular methods for uncertainty quantification such as perturbation
35 method [7, 8], point estimate method [9], simulation based approach [10, 11], Kriging
36 [12–17], polynomial chaos expansion [18, 19], moving least square method [20, 21] and
37 radial basis function [22–24] often yields erroneous results. For example, perturbation
38 method yields erroneous result for highly nonlinear system. This may be attributed
39 to the fact that since perturbation method utilizes a second order Taylor’s series ex-
40 pansion, it fails to capture the higher order of nonlinearity. Similar arguments hold
41 for point estimate method. In fact some of the most popular methods for uncertainty
42 quantification, *viz.*, Kriging, radial basis function, moving least square and PCE, suf-
43 fers from the curse of dimensionality. As a consequence, these methods may not be
44 applicable for problems involving large number of random variables. Even for lower
45 dimensional problems, the number of sample points required for Kriging is signifi-
46 cantly large. Simulation based approach, such as the crude Monte Carlo simulation
47 (MCS) is computationally expensive. Thus, stochastic methods, that are efficient as
48 well accurate, should be investigated.

49 This paper presents two novel approaches for solving RDO problems. The proposed ap-
50 proaches utilize polynomial correlated function expansion (PCFE) [25–31] for stochastic
51 computations and differential evolution algorithm (DEA) [32–35] for optimization. While
52 the first approach, referred to here as low-fidelity PCFE based DEA, yields a highly efficient
53 estimate of the RDO problems, the second variant, namely high-fidelity PCFE based DEA,
54 provides a highly accurate estimate for the RDO problems. Compared to exiting techniques
55 for RDO, the proposed approaches have certain desirable advantages.

- 56 • DEA is a global optimization tool and does not results in the local minima. Moreover,
57 it has already been established in previous studies [33] that DEA has rapid convergence
58 rate.

- 59 • DEA is a gradient-free optimization technique. Therefore, it is equally applicable to
60 both differentiable and non-differentiable functions.
- 61 • PCFE is an efficient uncertainty quantification tool capable of dealing with high di-
62 mensional problems. Thus, using PCFE to determine the statistical moments renders
63 the procedure highly efficient.

64 The rest of the paper is organised as follows. After describing the RDO problem in Section 2,
65 Section 3 describes the DEA utilized in this paper. In Section 4, a brief description of PCFE
66 has been provided. Section 5 introduces the proposed approaches for RDO. In Section 6
67 the proposed approach has been implemented for solving three examples. Section 7 presents
68 RDO of hydroelectric flow by using the proposed approaches. Finally, Section 8 provides the
69 concluding remarks.

70 2. Problem setup

71 RDO is the process of designing in the presence of uncertainty. It takes into account not only
72 the nominal value of input variables but also the uncertainties in those parameters whose
73 value is imprecisely known or is intrinsically variable. Mathematically, RDO is the process of
74 selecting the design variables while maximising the expected objective/goal function and/or
75 reducing its variance.

76 Suppose $\mathbf{x} := (x_1, x_2, \dots, x_N)$ be an \mathbb{R}^N valued input vector defined in probability space
77 $(\Omega, \mathcal{F}, \mathcal{P})$ and \mathbf{d} to be the design parameters. Then one possible description of RDO is [36]:

$$\begin{aligned}
 & \min_{\mathbf{d} \in \mathcal{D} \subseteq \mathbb{R}^N} c_0(\mathbf{d}) := f_o(E(y_0(\mathbf{x}, \mathbf{d})), \text{var}(y_0(\mathbf{x}, \mathbf{d}))) \\
 & \text{s.t.} \quad c_l(\mathbf{d}) := f_l(E(y_l(\mathbf{x}, \mathbf{d})), \text{var}(y_l(\mathbf{x}, \mathbf{d}))) \leq 0, \quad l = 1, 2, \dots, n_c \\
 & \quad \quad d_{i,L} \leq d_i \leq d_{i,U}, i = 1, 2, \dots, n_v
 \end{aligned} \tag{2}$$

78 where $E(\bullet)$ and $\text{var}(\bullet)$ denote mean and variance. It is evident from Eq. (2) that the objec-
79 tive function c_0 in RDO framework is represented as a function ($f_o(\bullet)$) of mean and standard
80 deviation of the objective function y_0 in deterministic/conventional optimization framework.
81 Similarly, the the constraints c_l in RDO are represented as a function ($f_l(\bullet)$) of mean and
82 standard deviation of the constraints y_l in deterministic/conventional optimization frame-

83 work. The above defined system is having n_c constraint function and n_v design variables.

84 $d_{i,L}$ and $d_{i,U}$ are, respectively, the lower and upper limits of i^{th} design vector.

85 In most applications, Eq. (2) is reformulated as [36, 37]

$$\begin{aligned} \min_{\mathbf{d} \in \mathbb{R}^N} \quad & c_0(\mathbf{d}) := \beta \frac{E(y_0(\mathbf{x}, \mathbf{d}))}{E(y_0(\mathbf{x}, \mathbf{d}))^*} + (1 - \beta) \frac{\sqrt{\text{var}(y_0(\mathbf{x}, \mathbf{d}))}}{\sigma_{y_0}^*} \\ \text{s.t.} \quad & c_l(\mathbf{d}) := E(y_l(\mathbf{x}, \mathbf{d})) + \kappa_l \sqrt{\text{var}(y_l(\mathbf{x}, \mathbf{d}))} \leq 0, \quad l = 1, 2, \dots, n_c \\ & d_{i,L} \leq d_i \leq d_{i,U}, \quad i = 1, 2, \dots, n_v \end{aligned} \quad (3)$$

86 where $\beta \in [0, 1]$ represents the weight. $E(y_0(\mathbf{x}, \mathbf{d}))^*$ and $\sigma_{y_0}^*$ are non-zero and real valued
87 scaling factors [36]. κ_l , $l = 1, 2, \dots, n_c$ are constant coefficients associated with constraint
88 functions. The focus of this work is to present the applicability of the proposed approaches
89 for solving the RDO problem described in Eq. (3).

90 3. Differential Evolution

91 Differential evolution algorithm (DEA) is a stochastic direct search method that optimizes
92 a problem by iteratively trying to improve a candidate solution with respect to a given
93 measure of quality. Unlike gradient based optimization, DEA does not use the gradient
94 of the problem and is thus equally applicable to both differentiable and non-differentiable
95 problems. Furthermore, DEA make few or no assumptions regarding the problem being
96 optimized and searches very large spaces of a candidate solution.

97 DEA utilizes n_P D -dimensional parameter vectors $x_{i,G}$, $i = 1, 2, \dots, n_P$ as a population for
98 each generation G . The initial vector population is considered to be uniformly distributed
99 over the entire parameter space. DEA generates new parameter vectors by adding the
100 weighted difference between the two population vectors to a third vector. This operation is
101 known as *mutation*. In the next step, the trial vector is obtained by mixing the parameter
102 vectors obtained after mutation with the target vector. This step is known as *crossover*.
103 If the magnitude of objective function obtained corresponding to the trial vector is smaller
104 compared to the target vector, trial vector replaces the target vector. This step is known as
105 *selection*. Note that each population vector must serve once as the target vector in order to
106 increase the competitions. Next, different steps of DEA have been described.

107 *3.1. Mutation*

108 For each target vector $x_{i,G}, i = 1, 2, \dots, n_P$, where G denotes generation, a mutant vector
 109 $v_{i,G+1}$, for the $G + 1^{\text{th}}$ generation, is generated as:

$$v_{i,G+1} = x_{k_1,G} + F \cdot (x_{k_2,G} - x_{k_3,G}) \quad (4)$$

110 where $k_1, k_2, k_3 \in \{1, 2, \dots, n_P\}$ are random integers that are mutually different. It is further
 111 ensured that k_1, k_2, k_3 are different from the running integer i . F is a real constant which
 112 controls the amplification of the differential variation $(x_{k_2,G} - x_{k_3,G})$. For further details,
 113 interested readers are referred to the work by [33].

114 *3.2. Cross-over*

115 The primary aim of this step is to increase the diversity of the perturbed parameter vectors.
 116 The trial vector $u_{i,G+1} = (u_{1i,G+1}, u_{2i,G+1}, \dots, u_{Di,G+1})$, having D candidates is formed, where

$$u_{ji,G+1} = \begin{cases} v_{ji,G+1} & \text{if } r_j \leq c_R \text{ or } j = \rho_i \\ x_{ji,G} & \text{if } r_j > c_R \text{ and } j \neq \rho_i \end{cases} \quad (5)$$

$\hat{j} = 1, 2, \dots, D$

118 In Eq. (5), r_j is the j^{th} uniform random number with outcome $\in [0, 1]$ and ρ_i is the randomly
 119 chosen index $\in 1, 2, \dots, D$. ρ_i ensures that $u_{i,G+1}$ gets at least one parameter from $v_{i,G+1}$.
 120 c_R is the crossover parameter and resides in $[0, 1]$. The value of c_R is to be provided by the
 121 user. For further details, readers may refer to the work by [33].

122 *3.3. Selection*

123 The final step of DEA is the selection. This step decides the suitability of trial vector. In this
 124 step, the trial vector $u_{i,G+1}$ is compared to the target vector $x_{i,G}$. If the value of objective
 125 function corresponding to $u_{i,G+1}$ is lower compared to that obtained using $x_{i,G}$, then $x_{i,G+1}$
 126 is set to be $u_{i,G+1}$. On contrary if, the value of objective function corresponding to $u_{i,G+1}$
 127 is greater compared to that obtained using $x_{i,G}$, then the old value of $x_{i,G}$ is retained. A
 128 flowchart depicting the procedure of DEA is shown in Fig. 1

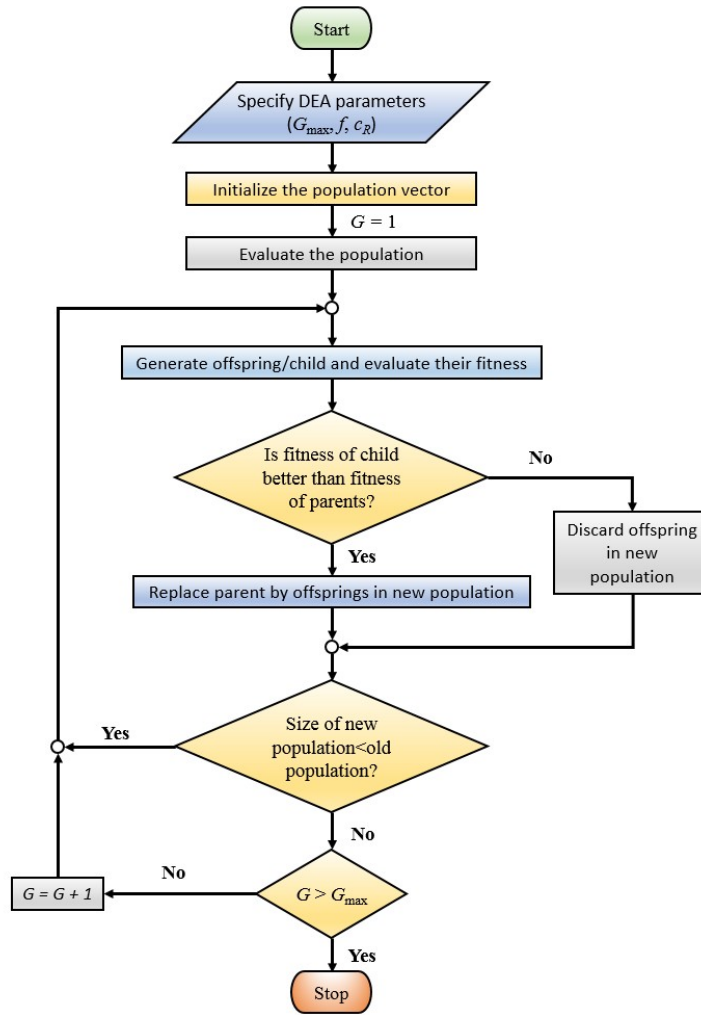


Figure 1: Flowchart for DEA

129 4. Foundation of PCFE

130 Polynomial correlated function expansion (PCFE) [25, 26] is a general set of quantitative
 131 model assessment and analysis tool for capturing high dimensional input-output system be-
 132 haviour. In literature, this method is also referred as generalised ANOVA [38] or generalised
 133 HDMR [39]. In this section, the mathematical formulation of PCFE has been discussed.

134 Let $\mathbf{i} = (i_1, i_2, \dots, i_N) \in \mathbb{N}_0^N$ be a multi-index with $|\mathbf{i}| = i_1 + i_2 + \dots + i_N$, and let $N \geq 0$ be
 135 an integer. Now considering $\mathbf{x} = (x_1, x_2, \dots, x_N)$ to be the random inputs, we express the

136 response of interest $g(\mathbf{x})$ as a series having finite number of terms as shown in Eq. (6)

$$g(\mathbf{x}) = \sum_{|\mathbf{i}|=0}^N g_{\mathbf{i}}(\mathbf{x}_{\mathbf{i}}) \quad (6)$$

137 *Definition 1: The univariate terms in Eq. (6) are termed as first order component functions.*

138 *Similarly, the bivariate terms, denoting cooperative effect of two terms acting together, are*
 139 *termed as second order component function.*

140 *Definition 2: Assume, two subspace R and B in Hilbert space are spanned by basis $\{r_1, r_2, \dots, r_l\}$*
 141 *and $\{b_1, b_2, \dots, b_m\}$ respectively. Now if (i) $B \supset R$ and (ii) $B = R \oplus R^\perp$ where, R^\perp is the or-*
 142 *thogonal complement subspace of R in B , we term B as extended basis and R as non-extended*
 143 *basis. [39]*

144 Now considering ψ to be a suitable basis of \mathbf{x} and utilizing definition 2, Eq. (6) can be
 145 rewritten as [25–28]

$$\hat{g}(\mathbf{x}) = g_0 + \sum_{k=1}^N \left\{ \sum_{i_1=1}^{N-k+1} \cdots \sum_{i_k=i_{k-1}}^N \sum_{r=1}^k \left[\sum_{m_1=1}^{\infty} \sum_{m_2=1}^{\infty} \cdots \sum_{m_r=1}^{\infty} \alpha_{m_1 m_2 \dots m_r}^{(i_1 i_2 \dots i_k) i_r} \psi_{m_1}^{i_1} \cdots \psi_{m_r}^{i_r} \right] \right\} \quad (7)$$

146 where α 's are the unknown coefficients associated with the bases and g_0 is a constant (termed
 147 as zeroth order component function). From practical point of view, the expression for PCFE
 148 provided in Eq. (7) needs to be truncated. Considering up to N_t^{th} order component function
 149 and s^{th} order basis yields:

$$\hat{g}(\mathbf{x}) = g_0 + \sum_{k=1}^{N_t} \left\{ \sum_{i_1=1}^{N-k+1} \cdots \sum_{i_k=i_{k-1}}^N \sum_{r=1}^k \left[\sum_{m_1=1}^s \sum_{m_2=1}^s \cdots \sum_{m_r=1}^s \alpha_{m_1 m_2 \dots m_r}^{(i_1 i_2 \dots i_k) i_r} \psi_{m_1}^{i_1} \cdots \psi_{m_r}^{i_r} \right] \right\} \quad (8)$$

150 *Definition 3: Eq. (8) is termed as N_t^{th} order PCFE expression. A N_t^{th} order PCFE consists*
 151 *of all the component functions up to N_t^{th} order, i.e., while first-order PCFE consists zeroth*
 152 *and first order component functions, a second-order PCFE consists zeroth, first and second*
 153 *order component functions. Therefore, adding all the N_t^{th} order component functions to an*
 154 *existing $(N_t - 1)^{\text{th}}$ order PCFE would yield the N_t^{th} order PCFE expression.*

155 As already illustrated in previous studies [26, 27], a second-order PCFE with third order
 156 basis yield satisfactory results for most practical cases. Hence, substituting $N_t = 2$ and

157 $s = 3$ in Eq. (8) yields:

$$g(\mathbf{x}) = g_0 + \sum_i \sum_k \alpha_k^{(i)i} \psi_k^i(x_i) + \sum_{1 \leq i < j \leq N} \left\{ \sum_{k=1}^3 \alpha_k^{(ij)i} \psi_k^i(x_i) + \sum_{k=1}^3 \alpha_k^{(ij)j} \psi_k^j(x_j) + \sum_{m=1}^3 \sum_{n=1}^3 \alpha_{mn}^{(ij)ij} \psi_m^i(x_i) \psi_n^j(x_j) \right\} \quad (9)$$

158 Rewriting Eq. (9) in matrix form

$$\mathbf{\Psi} \boldsymbol{\alpha} = \mathbf{e} \quad (10)$$

159 where $\mathbf{\Psi}$ consists of the basis functions and

$$\mathbf{e} = \mathbf{g} - \bar{\mathbf{g}} \quad (11)$$

160 where $\mathbf{g} = (g_1, g_2, \dots, g_{N_S})^T$ is a vector consisting of the observed responses at N_S sample
 161 points and $\bar{\mathbf{g}} = (g_0, g_0, \dots, g_0)^T$ is the mean response vector. Pre-multiplying Eq. (10) by
 162 $\mathbf{\Psi}^T$, one obtains

$$\mathbf{B} \boldsymbol{\alpha} = \mathbf{C} \quad (12)$$

163 where $\mathbf{B} = \mathbf{\Psi}^T \mathbf{\Psi}$ and $\mathbf{C} = \mathbf{\Psi}^T \mathbf{e}$. Close inspection of $\mathbf{\Psi}$ reveals identical columns. Thus,
 164 \mathbf{B} has identical rows. These rows are redundant and can be removed. Removing identical
 165 rows of \mathbf{B} and corresponding rows of \mathbf{C} , one obtains

$$\mathbf{B}' \boldsymbol{\alpha}' = \mathbf{C}' \quad (13)$$

166 where \mathbf{B}' and \mathbf{C}' are respectively, \mathbf{B} and \mathbf{C} after removing the redundants.

167 **Remark 1:** An essential condition, associated with Eq. (13) is the hierarchical orthogonality
 168 of the component functions. This condition requires a higher order component function to
 169 be orthogonal with all the lower order component functions. To determine the unknown
 170 coefficients $\boldsymbol{\alpha}$ while satisfying the orthogonality criteria, homotopy algorithm (HA) [40–43] is
 171 employed. HA determines the unknown coefficients associated with the bases by minimizing
 172 the least-squared error and satisfying the hierarchical orthogonality criteria.

173 4.1. Homotopy algorithm

174 Consider \mathbf{B}' to be a $p \times q$ matrix. Since the system described by Eq. (13) is underdetermined,
 175 there exists an infinite number of solution given by

$$\boldsymbol{\alpha}(s) = (\mathbf{B}')^{-1} \mathbf{C}' + \left[\mathbf{I} - (\mathbf{B}')^{-1} \mathbf{B}' \right] v(s) \quad (14)$$

176 where $(\mathbf{B}')^{-1}$ denotes the generalized inverse of \mathbf{B}' , $v(s)$ is an arbitrary vector in \mathbb{R}^q and \mathbf{I}
 177 represents an identity matrix. One choice of $(\mathbf{B}')^{-1}$ in Eq. (14) is $(\mathbf{B}')^\dagger$, which is the the
 178 generalised inverse of \mathbf{B}' satisfying all four Penrose conditions [44]. The solution of $\boldsymbol{\alpha}(s)$
 179 after replacing $(\mathbf{B}')^{-1}$ by $(\mathbf{B}')^\dagger$ is given as

$$\begin{aligned}\boldsymbol{\alpha}(s) &= (\mathbf{B}')^\dagger \mathbf{C}' + [\mathbf{I} - (\mathbf{B}')^\dagger \mathbf{B}'] v(s) \\ &= (\mathbf{B}')^\dagger \mathbf{C}' + \mathbf{P} v(s)\end{aligned}\quad (15)$$

180 It is noted that \mathbf{P} is an orthogonal projector and satisfies

$$\mathbf{P}^2 = \mathbf{P}, \quad \mathbf{P}^T = \mathbf{P}\quad (16)$$

181 All the solutions of $\boldsymbol{\alpha}$ obtained from Eq. (15) compose a completely connected submanifold
 182 $\mathcal{M} \subset \mathbb{R}^q$. Homotopy algorithm searches for the best solution by considering an exploration
 183 path $\boldsymbol{\alpha}(s)$ within \mathcal{M} with $s \in [0, \infty)$, which satisfies

$$\frac{d\boldsymbol{\alpha}(s)}{ds} = \mathbf{P}\mathbf{v}'\quad (17)$$

184 where $\mathbf{v}' = d\mathbf{v}/ds$. The free function vector \mathbf{v}' may be chosen freely to enable broad choices
 185 for exploring $\boldsymbol{\alpha}(s)$ and provide the possibility to continuously reduce the predefined cost
 186 function.

187 The cost function in homotopy algorithm is defined as

$$O = \frac{1}{2} \boldsymbol{\alpha}^T \mathbf{W} \boldsymbol{\alpha}\quad (18)$$

188 where \mathbf{W} is the weight matrix which is symmetric and non-negative definite. Minimizing
 189 the cost function is the additional condition that is imposed on homotopy algorithm. Con-
 190 sidering,

$$\mathbf{v}' = -\frac{\partial O}{\partial \mathbf{a}(s)}\quad (19)$$

191 and noting that \mathbf{P} is an orthogonal projector, we obtain

$$\begin{aligned}\frac{\partial O}{\partial s} &= \left(\frac{\partial O}{\partial \boldsymbol{\alpha}(s)} \right) \left(\frac{\partial \boldsymbol{\alpha}(s)}{\partial s} \right) = \left(\frac{\partial O}{\partial \boldsymbol{\alpha}(s)} \right) \mathbf{P}\mathbf{v}' \\ &= -\left(\mathbf{P} \frac{\partial O}{\partial \boldsymbol{\alpha}(s)} \right)^T \left(\mathbf{P} \frac{\partial O}{\partial \boldsymbol{\alpha}(s)} \right) \\ &\leq 0\end{aligned}\quad (20)$$

192 From Eq. (20), it is obvious that the objective function O is minimized as $s \rightarrow \infty$. The

193 solution of Eq. (17), obtained using homotopy algorithm is given as

$$\boldsymbol{\alpha}_{HA} = \left[\mathbf{V}_{q-r} (\mathbf{U}_{q-r}^T \mathbf{V}_{q-r})^{-1} \mathbf{U}_{q-r}^T \right] \boldsymbol{\alpha}_0 \quad (21)$$

194 where $\boldsymbol{\alpha}_0$ is the solution obtained using least-squares regression. \mathbf{U}_{q-r} and \mathbf{V}_{q-r} are the last
195 $q - r$ columns of \mathbf{U} and \mathbf{V} obtained from singular value decomposition of matrix \mathbf{PW} .

$$\mathbf{PW} = \mathbf{U} \begin{pmatrix} \mathbf{A}_r & 0 \\ 0 & 0 \end{pmatrix} \mathbf{V}^T \quad (22)$$

196 Eq. (21) is the key formula for determining the optimal solution of $\boldsymbol{\alpha}$ from homotopy algo-
197 rithm. A detailed derivation of the same can be found in [25, 27, 39].

198 **Remark 2:** An important aspect for HA is the formulation of weight matrix. A detailed
199 description of weight matrix, based on the hierarchical orthogonality criteria, is provided in
200 Appendix A.

201 A step-by-step procedure for PCFE is shown in Algorithm 1.

202 5. Proposed approach for robust optimization

203 PCFE, described in previous section, provides an efficient means to approximate the objective
204 and constraint functions. However, there exists multiple alternatives for coupling PCFE, into
205 the framework of an optimization algorithm (DEA in this case). Two such alternatives are
206 presented in this section.

207 5.1. Low-fidelity PCFE based DEA

208 This approach involves a straightforward integration of PCFE into DEA. However, instead
209 of generating a PCFE model at each design step, a single PCFE model is generated at the
210 onset and the same model is utilized for all the iterations of DEA. As a consequence, the
211 computational effort involved in this step is minimal. The steps involved in low-fidelity
212 PCFE based DEA are outlined below.

213 **Step1:** Determine lower limit and upper limit of the design variables. Suppose $d_{i,l}$ and $d_{i,u}$
214 be the bounds of the design variables. Also assume, δ to be the coefficient of variation.

Algorithm 1: Algorithm of PCFE

1. **INITIALIZE:** Provide distribution type and distribution parameters of the input random variables. Identify bounds of random variables.
2. Input *order* of PCFE
3. Input number (*num*) of sample points;
4. Obtain responses at sample points
5. $g_0 \leftarrow \frac{1}{num} \sum_s g(x_s)$ where *num* is the number of sample points
6. **for** $i = 1 : num$
 $e_i \leftarrow g(x_i) - g_0$
end for
7. $\Psi \leftarrow \left[\psi(\mathbf{x}^1) \quad \psi(\mathbf{x}^2) \quad \cdots \quad \psi(\mathbf{x}^N) \right]^T$ where

$$\psi(\mathbf{x}^r)^T \leftarrow \left[\begin{array}{ccccccc} \psi_1^1(x_1^r) & \psi_2^1(x_1^r) & \cdots & \psi_k^1(x_1^r) & \psi_1^2(x_2^r) & \cdots & \\ & \psi_1^1(x_1^r) & \cdots & \psi_m^{N-2}(x_{N-2}^r) & \psi_m^{N-1}(x_{N-1}^r) & & \\ & & & \psi_m^{N-1}(x_{N-1}^r) & \psi_m^N(x_N^r) & & \end{array} \right]$$
8. $\mathbf{e} \leftarrow \left[e_1 \quad e_2 \quad \cdots \quad e_n \right]^T$
9. $[\mathbf{B}', \mathbf{C}'] \leftarrow \text{remove_redundants}(\mathbf{B}, \mathbf{C})$
10. $\mathbf{W} \leftarrow \text{form_weight}(\psi)$
11. Utilize HA to determine the unknown coefficients
12. Obtain statistical moments of the response

Then the lower limit $d_{i,ll}$ and upper limit $d_{i,ul}$ are defined as:

$$d_{i,ll} = d_{i,l} (1 - \gamma\delta)$$

$$d_{i,ul} = d_{i,u} (1 + \gamma\delta)$$

For present study, $\gamma = 3$ has been considered. Similarly, set the lower limit and upper limit of other stochastic variables (apart from the design variables).

Step 2: Using Algorithm 1, formulate a PCFE model $\in [d_{i,ll}, d_{i,ul}]$ for the objective function y_0 . Similarly, formulate PCFE model(s) for constraint function(s) y_l as well. Formulate objective and constraint functions for the RDO problem by substituting y_0 with \tilde{y}_0

221 and y_l with \tilde{y}_l in Eq. (3), where \tilde{y}_0 and \tilde{y}_l are PCFE models representing y_0 and y_l
 222 respectively.

223 **Step 3:** Optimize the RDO problem defined in Step 2 using DEA.

224 5.2. High-fidelity PCFE based DEA

225 Although the low-fidelity PCFE based DEA is highly efficient, it may yield erroneous result
 226 specifically for problems involving higher order of nonlinearity, either in objective function
 227 or in constraints. One possible alternative is to generate PCFE models for the objective and
 228 constraint functions at each iteration. However, such an approach renders the procedure
 229 computationally expensive, making it unsuitable for large scale problems. In this work, an
 230 alternative high-fidelity approach has been presented. The proposed approach memorizes
 231 the previously generated PCFE model and utilizes them in the optimization step. The steps
 232 involved in the proposed high-fidelity PCFE based DEA are outlined below.

233 **Step 1:** Following the steps for low-fidelity PCFE based DEA, generate PCFE models for
 234 the objective and constraint functions.

235 **Step 2:** Define error tolerance ϵ . Also select an initial design vector. Set $i = 0$ and $j_l =$
 236 $0, l = 1, 2, \dots, n_c$.

237 **Step 3:** Compute the objective function y_0 and constraint functions y_l at the design point.
 238 Using the PCFE models, compute $\tilde{y}_{0,0}$ and $\tilde{y}_{l,0}$ at the design points.

239 **Step 4:** temp = 0

240 **for** $k = 0 : i$
 241 **if** $\left| \frac{y_0 - \tilde{y}_{0,k}}{y_0} \right| \leq \epsilon$

242 In Eq. (3), replace y_0 with $\tilde{y}_{0,k}$

243 **else**

244 **set** temp=temp + 1

245 **end if**

246 **if** temp= $i + 1$

247 **set** $i = i + 1$. Generate a local PCFE based model for the objective function $\tilde{y}_{0,i}$,

248 anchored around the design point.

249 In Eq. (3), replace y_0 with $\tilde{y}_{0,i}$.

250 **end if**

251 **end for**

252 **Step 5: for** $l = 1 : n_c$

253 temp1 = 0

254 **for** $k = 1 : j_l$

255 **if** $\left| \frac{y_l - \tilde{y}_l}{y_{l,k}} \right| \leq \varepsilon$

256 In Eq. (3), replace y_l with $\tilde{y}_{l,k}$

257 **else**

258 **set** temp1=temp1+1

259 **end if**

260 **if** temp1= $j_l + 1$

261 **set** $j_l = j_l + 1$. Generate a PCFE model for the constraint \tilde{y}_{l,j_l} , anchored about the
262 design point.

263 In Eq. (3), replace y_l with \tilde{y}_{l,j_l} .

264 **end if**

265 **end for**

266 **end for**

267 **Step 6** Obtain updated design vector. If solution is converged, **stop**. Else **go to** Step 3.

268 A flowchart depicting the two proposed approach are shown in Fig. 2.

269 6. Numerical Examples

270 In this section, three examples are presented to illustrate the proposed approaches for RDO.

271 While a mathematical function has been considered in Example 1, Example 2 illustrates

272 the implementation of DEA-PCFE for RDO of a simple truss. In example 3, RDO of

273 a transmission tower has been performed. For all the problems, the population size and

274 the generation size in DEA are considered to be 50 and 100 respectively. The cross-over

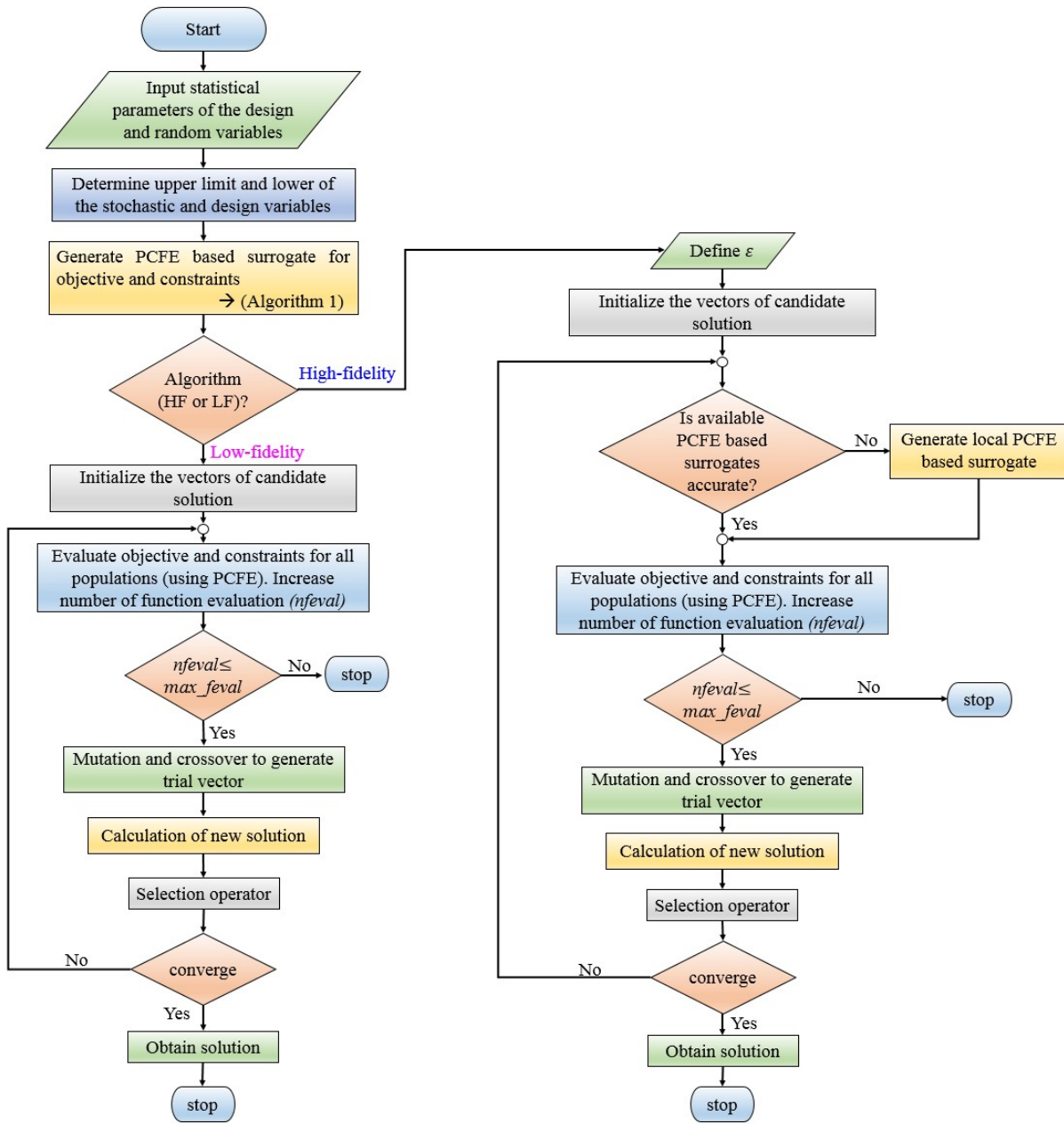


Figure 2: Flowchart for the proposed approaches

275 parameter is considered to be 0.5. The mutation parameter F is considered to be 0.8. The
 276 sample points required for PCFE are generated using Sobol sequence [45, 46]. However, it
 277 is worth mentioning that DEA-PCFE is equally applicable with both uniformly and non-
 278 uniformly distributed sample points.
 279 For ease of understanding, high-fidelity PCFE based DEA has been denoted as HF DEA-

280 PCFE. Similarly, low-fidelity PCFE based DEA is denoted as LF DEA-PCFE.

281 6.1. Example 1: optimization of a mathematical function [47]

282 This example illustrates the performance of DEA-PCFE for RDO of an explicit mathematical
283 function [47]. The problem involves two independent Gaussian random variables X_1 and X_2
284 and two design variables $d_1 = E(X_1)$ and $d_2 = E(X_2)$. The RDO problem reads

$$\begin{aligned} \min_{\mathbf{d} \in D} \quad & c_O(\mathbf{d}) = \frac{\sigma_{\mathbf{d}}(y_0(\mathbf{X}))}{15} \\ \text{s.t.} \quad & c_k(\mathbf{d}) = 3\sigma_{\mathbf{d}}(y_1(\mathbf{X})) - E(y_1(\mathbf{X})) \\ & 1 < d_1, d_2 < 10 \end{aligned} \quad (23)$$

285 where the two functions $y_0(\mathbf{X})$ and $y_1(\mathbf{X})$ are given as

$$y_0(\mathbf{X}) = (X_1 - 4)^3 + (X_1 - 3)^4 + (X_2 - 5)^2 + 10 \quad (24)$$

286 and

$$y_1(\mathbf{X}) = X_1 + X_2 - 6.45 \quad (25)$$

287 The standard deviation of both X_1 and X_2 is 0.4.

288 The proposed approaches have been utilized for solving this problem. Table 1 shows the opti-
289 mum design obtained using the proposed approaches. Results obtained have been compared
290 with results presented in [47] and Kriging. It is observed that DEA-PCFE ($c_O(\mathbf{d}^*) = 0.074$)
291 outperforms popular RDO techniques, such as tensor product quadrature (TPQ) ($c_O(\mathbf{d}^*) =$
292 0.086), Taylor's series (TS) ($c_O(\mathbf{d}^*) = 0.090$) and Kriging ($c_O(\mathbf{d}^*) = 0.076$). Moreover,
293 number of actual simulation required using the proposed approaches ($N_s = 76/84$) are sig-
294 nificantly less as compared to TPQ ($N_s = 162$), TS ($N_s = 90$) and Kriging ($N_s = 256$).

295 Another interesting aspect observed from Table 1 is that both the proposed approaches,
296 i.e. LF DEA-PCFE and HF DEA-PCFE yields identical result. This is because in all the
297 iterations, the initial PCFE model is found to yield satisfactory results. The additional
298 sample points required in HF DEA-PCFE is because of the additional simulations required,
299 at each iteration, to verify the accuracy of the initial PCFE model.

300 6.2. Example 2: 2-bar truss

301 In this example, a 2-bar truss element, as shown in Fig. 3, has been considered [47]. The
302 system is having five independent random variables, namely cross-sectional area X_1 , the

Table 1: Optimized parameters for Example 1

Methods	d_1^*	d_2^*	$c_O(\mathbf{d}^*)$	$N_s^\#$	
TPQ ¹	3.45	5.00	0.086	162 (81+81)	
TS ²	3.50	4.99	0.090	90 (45+45)	
Kriging	3.37	5.00	0.076	256 (128+128)	
DEA-PCFE	LF	3.35	4.99	0.074	76 (52+24)
	HF	3.35	4.99	0.074	82 (56+28)

¹Tensor product quadrature, ²Taylor's series

#The two numbers in bracket indicates simulations required for approximating y_0 and y_1 respectively.

303 horizontal span (half) X_2 , material density X_3 , load X_4 and tensile strength X_5 . The details
 304 of random variables are provided in Table 2. The design variables are $d_1 = E(X_1)$ and
 305 $d_2 = E(X_2)$. The objective of this problem is to minimize the second moment properties of
 306 mass of the structure given limiting stresses in both members are below the material yield
 307 stress. Consequently, the RDO problem is formulated as:

$$\begin{aligned}
 \min_{\mathbf{d} \in D} \quad & c_O(\mathbf{d}) = \beta_1 \frac{E(y_0(\mathbf{X}))}{10} + (1 - \beta_1) \frac{\sigma(y_0(\mathbf{X}))}{2} \\
 \text{s.t.} \quad & c_1(\mathbf{d}) = 3\sigma(y_1(\mathbf{X})) - E(y_1(\mathbf{X})) \leq 0 \\
 & c_2(\mathbf{d}) = 3\sigma(y_2(\mathbf{X})) - E(y_2(\mathbf{X})) \leq 0 \\
 & 0.2 \text{ cm}^2 \leq d_1 \leq 20 \text{ cm}^2, \quad 0.1 \text{ m} \leq d_2 \leq 1.6 \text{ m}
 \end{aligned} \tag{26}$$

308 where y_0, y_1 and y_2 are respectively mass of the structure, stress in member 1 and stress in
 309 member 2.

310 Table 3 shows the RDO results obtained using DEA-PCFE, TPQ, TS and Kriging. It is
 311 observed that LF DEA-PCFE ($c_O(\mathbf{d}^*)=1.189$, $N_s = 320$) outperforms TPQ ($c_O(\mathbf{d}^*)=1.239$,
 312 $N_s = 7722$) and Kriging ($c_O(\mathbf{d}^*)=1.37$, $N_s = 1280$), both in terms of accuracy and efficiency.
 313 HF DEA-PCFE and TS yields the best results ($c_O(\mathbf{d}^*)=1.174$). However, number of function
 314 evaluations using HF DEA-PCFE ($N_s = 640$) is less, as compared to TS ($N_s = 648$).

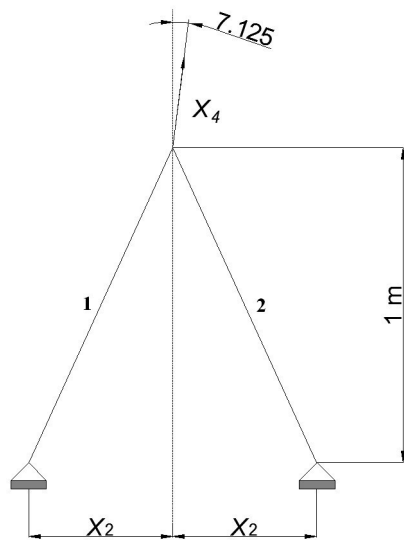


Figure 3: 2-bar truss structure considered in Example 2

Table 2: Properties of random variables

Variable	Mean	COV	type
X_1	d_1	0.02	Gaussian
X_2	d_2	0.02	Gaussian
X_3	10000	0.2	Beta*
X_4	800	0.25	Gumbel
X_5	1050	0.24	lognormal

*For beta distribution, both parameters are 5.

315 6.3. Example 3: a transmission tower

316 In this example, the performance of the proposed approaches in robust design optimization
 317 of a transmission tower [48, 49] has been illustrated. Fig. 4 shows a schematic diagram of
 318 the transmission tower. The structure is modelled using truss elements. It is subjected to
 319 lateral and vertical loads. The location of the loads are shown in Fig. 4. The first four
 320 nodal forces, namely P_1 , P_2 , P_3 and P_4 are having magnitude -1.0×10^4 . The other two
 321 loads are considered to be random. Apart from the two loads, the material and geometric
 322 properties are also considered random. As a consequence, the system is having fourteen
 323 random variables. Group membership of the twenty five members and the parameters of the

Table 3: Robust design of Example 2

Methods	d_1^*	d_2^*	$c_O(\mathbf{d}^*)$	$N_s^\#$
TPQ ¹	11.567	0.3767	1.239	7722 (594+2×3564)
TS ²	10.957	0.3770	1.174	648 (108+2×270)
Kriging	12.783	0.3770	1.37	1280 (256+2×512)
DEA-PCFE	LF	11.087	0.3810	320 (64+2×128)
	HF	10.958	0.3770	640 (128+256+256)

¹Tensor product quadrature, ²Taylor's series

#The three numbers in bracket indicates simulations required for approximating y_0 , y_1 and y_2 respectively.

324 random variables are shown in Table 4 and Table 5, respectively. In accordance with [48],
 325 all the random variables are assumed to be normally distributed. The design variables are
 assumed to be bounded in $[0.05, 10]$.

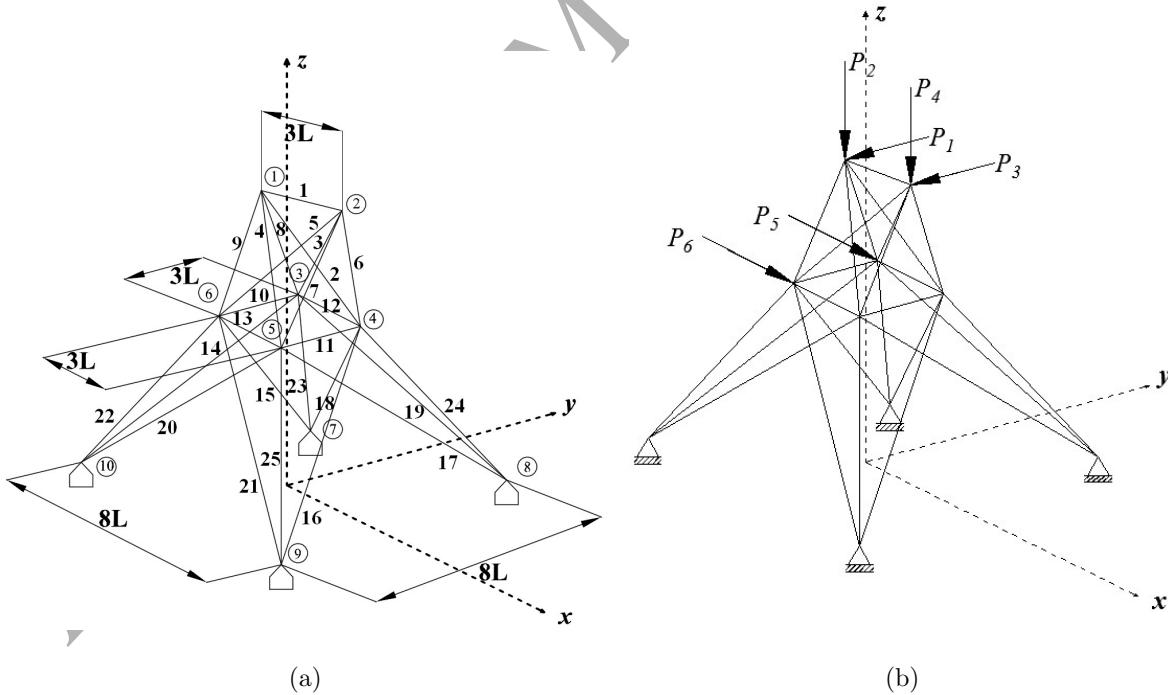


Figure 4: Schematic diagram of transmission tower : (a) dimensional details along with node and element numbers, (b) loading details

Table 4: Group members for the transmission tower

Group number	Members
I	1
II	2,3,4,5
III	6,7,8,9
IV	10,11,12,13
V	14,15,16,17,18,19,20,21
VI	22,23,24,25

Table 5: Random variables for the transmission tower

Sl	Variables	Type	Mean	SD	COV
1 - 5	$E_I - E_V$	Normal	1.0×10^7	2.0×10^5	
6	E_{VI}	Normal	1.0×10^7	1.5×10^6	
7	P_5	Normal	500	50	
8	P_6	Normal	500	50	
9 - 14	$A_I - A_{VI}$	Normal			0.05

327 The optimization problem reads

$$\begin{aligned}
\min_{\mathbf{d} \in \mathbb{R}^6} \quad & c_0(\mathbf{d}) := \beta \frac{E(y_0)}{E(y_0)^*} + (1 - \beta) \frac{\sqrt{\text{var}(y_0)}}{\sigma_{y_0}^*} \\
\text{s.t.} \quad & c_i(\mathbf{d}) := E(|s_i|) + 3\sigma_{s_i} \leq s_{max}, \quad i = 1, 2, \dots, 25 \\
& c_{26}(\mathbf{d}) := E(w) \leq 750 \\
& 0.05 \leq \mathbf{d} = [A_I, A_{II}, \dots, A_{VI}] \leq 10
\end{aligned} \tag{27}$$

328 where y_0 denotes the structural compliance ($\mathbf{P}^T \mathbf{U}$) and s_i denotes the stress generated in the
329 i^{th} member. β and w , respectively, denote weighing factor for RDO and the structural weight.
330 \mathbf{P} and \mathbf{U} in the expression of elastic compliance denote the force vector and displacement
331 vector respectively. s_{max} denotes the maximum allowable stress in the truss members and σ
332 denotes the standard deviation. In accordance with the actual problem definition provided
333 by [48], $s_{max} = 5000$ has been considered.

334 The proposed approaches have been utilized to solve the problem. The cross-over parameter

335 and the mutation parameter F are considered to be 0.5 and 0.8, respectively. Benchmark
 336 solution for this problem has been generated by coupling MCS with DEA. Table 6 depicts
 337 the results obtained using various methods. Case studies by considering different values of
 338 β has also been reported. For all the cases, the benchmark solution obtained using DEA-
 339 MCS and the proposed HF DEA-PCFE are in close proximity. On the other hand, results
 340 obtained using LF DEA-PCFE deteriorate from the benchmark solution. This is because a
 341 single PCFE model fails to capture the second moment properties of the response. Kriging
 342 is also found to yield erroneous results.

343 Results reported in [48] are significantly different from those obtained in this study. This
 344 is because, the optimum design variables reported in [48] violates the stress constraint in
 345 member 13. Similar observation has also been stated in [50].

346 As for the computational cost associated, LF DEA-PCFE is the most efficient followed by
 347 HF DEA-PCFE and Kriging. This is because while LF DEA-PCFE operates based on a
 348 single PCFE model, HF DEA-PCFE builds several local PCFE models.

349 Next, in order to allow the solutions obtained by Doltsinis and kang [48] to be valid,
 350 $s_{max} = 12,5000$ has been considered [50]. The solutions obtained with this setup are re-
 351 ported in Table 7. It is observed that the proposed HF DEA-PCFE yields excellent results
 352 outperforming Kriging based RDO and method proposed in [48]. In fact, LF DEA-PCFE
 353 also yields satisfactory results and that to from significantly reduced computational cost.

354 7. Application: robust hydroelectric flow optimization

355 Over the last decade or so, several hydropower generation models have been investigated by
 356 scientists. While some of the models were analytical, others were constructed from robust
 357 system models showing the dynamic characteristics. A detailed account of various models of
 358 hydro plant and techniques used to control generation of power has been shown in [51, 52].

359 7.1. Model definition

360 Considering $f_t(i)$ and $S_i(i)$ to be the flow through turbine and storage level of the reservoir
 361 at the i^{th} hour, the electricity produced at the i^{th} hour is computed as:

$$E(i) = f_t(i-1) [0.5k_1 \{S(i) + S(i-1)\} + k_2] \quad (28)$$

Table 6: Robust designs of transmission tower. $s_{max} = 5000$ has been considered

β	Methods	A_I	A_{II}	A_{III}	A_{IV}	A_V	A_{VI}	$E(y_0)$	σ_{y_0}	N_s^*
0	DEA-MCS	0.05	0.05	4.48	2.16	0.79	7.04	5547.7	347.4	1.64×10^6
	Kriging [#]	2.24	2.11	2.86	1.98	1.57	4	6249.9	467.94	2500
	Past work [#] [48]	0.147	0.672	3.465	0.566	0.822	8.048	6196	295	-
	DEA- LF	0.05	0.05	4.16	3.96	0.95	5.45	5914.8	422.5	1024
	PCFE HF	0.05	0.05	4.49	2.16	0.79	7.03	5550.7	347.73	2432
	DEA-MCS	0.05	0.05	4.48	2.15	0.79	7.04	5547.7	347.4	1.64×10^6
0.25	Kriging [#]	0.28	0.75	3.48	1.23	1.26	6.39	5685.4	339.86	2500
	Past work [#] [48]	0.114	0.558	3.685	0.575	0.925	7.704	6036	297	-
	DEA- LF	0.05	0.05	4.16	3.96	0.95	5.45	5914.8	422.5	1024
	PCFE HF	0.05	0.05	4.48	2.16	0.79	7.04	5550.7	347.73	2432
	DEA-MCS	0.05	0.05	4.48	2.10	0.89	6.81	5499.2	349.7	1.64×10^6
	Kriging [#]	0.05	0.05	4.43	1.53	1.23	6.23	5476.8	347.01	2500
0.5	Past work [#] [48]	0.05	0.207	4.28	0.628	1.15	6.94	5775	304	-
	DEA- LF	0.05	0.05	5.16	2.43	1.15	5.15	5504	411.21	1024
	PCFE HF	0.05	0.05	4.48	2.09	0.90	6.78	5496.30	350.33	2168
	DEA-MCS	0.05	0.05	4.91	2.02	0.98	6.26	5386.30	363.27	1.64×10^6
	Kriging [#]	0.05	0.05	5.05	1.58	1.13	5.98	5362.6	360.3	2500
	Past work [#] [48]	0.05	0.075	4.88	0.95	1.18	6.33	5478	330	-
0.75	DEA- LF	0.05	0.05	4.76	2.47	1.13	5.56	5502.3	391.85	1024
	PCFE HF	0.05	0.05	4.91	2.01	0.99	6.24	5286.3	363.76	1986
	DEA-MCS	0.05	0.05	5.62	1.62	1.05	5.71	5333.30	387.46	1.64×10^6
	Kriging [#]	0.05	0.05	5.62	1.62	1.05	5.71	5327.9	386.27	2500
	Past work [#] [48]	0.05	0.05	5.74	1.718	1.054	5.574	5328	384	-
	DEA- LF	0.05	0.05	6.14	2.38	1.02	4.76	5526.5	444.59	1024
1.0	PCFE HF	0.05	0.05	5.6	1.96	1.03	5.61	5333.3	387.46	1668

*No. of actual simulations

#Constraints not satisfied

Table 7: Robust designs of transmission tower. $s_{max} = 12,500$ has been considered

β	Methods	A_I	A_{II}	A_{III}	A_{IV}	A_V	A_{VI}	$E(y_0)$	σ_{y_0}	N_s^*
0	DEA-MCS	0.36	0.97	2.50	0.40	1.07	7.91	6498	291.69	1.64×10^6
	Kriging [#]	0.27	1.12	2.87	0.36	1.09	8.14	6056	275.39	2500
	Past work [48]	0.147	0.672	3.465	0.566	0.822	8.048	6196	295	-
	DEA- LF	0.29	0.86	2.75	0.41	1.15	7.55	6351	293.65	1024
	PCFE HF	0.31	0.85	2.63	0.42	1.10	7.83	6452	291	2218
	DEA-MCS	0.20	0.58	3.41	0.47	1.20	7.19	6045	295.15	1.64×10^6
0.25	Kriging	0.14	0.42	3.58	0.49	1.24	7.10	6012	296.08	2500
	Past work [48]	0.114	0.558	3.685	0.575	0.925	7.704	6036	297	-
	DEA- LF	0.18	0.55	3.35	0.52	1.22	7.1	6064	300.44	1024
	PCFE HF	0.19	0.53	3.49	0.48	1.22	7.20	6001	294.21	2072
	DEA-MCS	0.05	0.10	4.44	0.55	1.27	6.62	5769	303.88	1.64×10^6
	Kriging	0.05	0.06	4.48	0.55	1.29	6.57	5769	304.35	2500
0.5	Past work [48]	0.05	0.207	4.28	0.628	1.15	6.94	5775	304	-
	DEA- LF	0.05	0.1	4.46	0.57	1.25	6.48	5804	310.41	1024
	PCFE HF	0.05	0.12	4.46	0.55	1.28	6.59	5746	304	1854
	DEA-MCS	0.05	0.05	5.02	1.11	1.08	6.41	5435	337.87	1.64×10^6
	Kriging [#]	0.05	0.05	5.03	1.13	1.14	6.33	5389	337	2500
	Past work [48]	0.05	0.075	4.88	0.95	1.18	6.33	5478	330	-
0.75	DEA- LF	0.05	0.05	4.97	1.12	0.99	6.28	5591	349.28	1024
	PCFE HF	0.05	0.05	5.02	1.10	1.09	6.39	5438	337.28	1648
	DEA-MCS	0.05	0.05	5.67	1.66	1.05	5.67	5324	379.51	1.64×10^6
	Kriging [#]	0.05	0.05	5.70	1.64	1.10	5.72	5252	373.01	2500
	Past work [48]	0.05	0.05	5.74	1.718	1.054	5.574	5328	384	-
	DEA- LF	0.05	0.05	5.73	1.72	1.04	5.58	5338	385.53	1024
1.0	PCFE HF	0.05	0.05	5.67	1.66	1.04	5.67	5327	379.79	1442

*No. of actual simulations

#Constraints not satisfied

362 where $k_1 = 0.00003$ is termed as K-factor coefficient and $k_2 = 9$ is termed as K-factor offset
 363 [53]. The hourly storage level $S(i)$ is again computed as:

$$S(i) = S(i-1) + \Delta t [f_i(i-1) - f_s(i-1) - f_t(i-1)] \quad (29)$$

364 where $f_i(\bullet)$ and $f_s(\bullet)$, respectively, denote the in-flow and flow through spillway. Once
 365 the hourly electricity generated is computed using Eq. (28) and Eq. (29), hourly revenue
 366 generated from the dam is computed as:

$$R_i = E(i) P(i) \quad (30)$$

367 where R_i is the hourly revenue generated and $P(i)$ denotes the hourly electricity price. Now
 368 if R is the total revenue generated by the dam, then

$$R = \sum_i R_i \quad (31)$$

369 From Eq. (28) - Eq. (31), it is clear that electricity generation using a hydroelectric dam
 370 is primarily governed by the hourly water supplied through the turbine and the water level
 371 in the reservoir. It is quite obvious that due to environmental variations, large amount of
 372 uncertainties are associated with a hydroelectric dam. Moreover, hourly cost of electricity
 373 (P_i) is also influenced by various factors. Hence, it is of utter importance to consider the
 374 presence of uncertainties while optimizing (maximising) the overall revenue (R) of a hy-
 375 droelectric dam. Fig. 5 shows a schematic diagram of hydroelectric dam considered in the
 376 present study. Conventional optimization of the above mentioned hydroelectric dam can be
 377 found in [53].

378 Various uncertainties are associated with any hydroelectric dam. For instance, the flow
 379 through spillway (f_s) and turbine (f_t) are generally controlled by some machine operated
 380 gates. However, it is not possible to exactly control the flow with such machineries and
 381 this results in some uncertainties. On the other hand, the in-flow (f_i) to the reservoir is
 382 uncontrolled and hence large sources of uncertainties is associated with this. Moreover,
 383 market price of electricity depends on various factors and is highly uncertain. It is to be
 384 noted that f_s , f_t , f_i and market price P_i are generally monitored on an hourly basis. In the
 385 present study, the simulation is run for 12 hours and hence, the **system** under consideration
 386 involves 48 random variables. A detailed account of the involved uncertain variables have

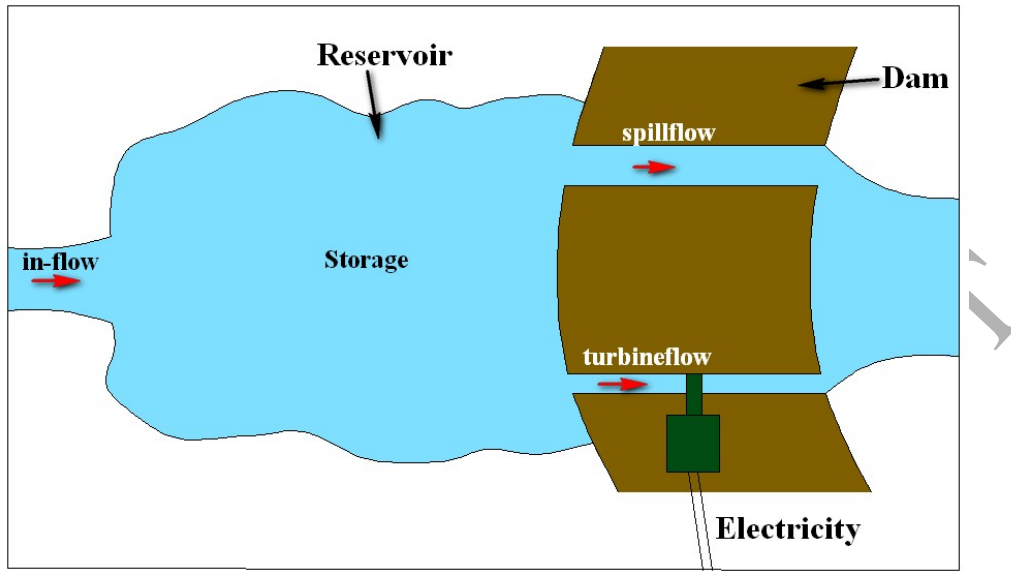


Figure 5: Schematic diagram of hydroelectric dam

been provided in Table 8.

Table 8: Statistical parameters of the uncertain inputs

Sl. No.	Variable	Distribution	Mean	COV/SD
1 - 12	hourly in-flow	Normal	1070 CFS	0.05
13 - 24	hourly electricity price	Normal	45 CFS	0.3
25 - 36	hourly flow through turbine	Lognormal	-	100* CFS
37 - 48	hourly flow through spillway	Lognormal	-	0.02

* indicates standard deviation

CFS = cubic feet per second

387

388 7.2. Problem definition

389 The electricity produced in a hydroelectric dam depends on two primary parameters, namely
 390 amount of water flowing through the turbine and the reservoir storage level. The storage of
 391 reservoir again depends on the three factors: (a) in-flow, (b) flow through turbine and (c) flow
 392 through spillway. As the flow through turbine increases, the water in the reservoir decreases.
 393 Therefore, it is necessary to compute the optimum flow through the turbine and spillway that
 394 maximises the electricity production. Moreover, certain constraints needs to be considered

395 while solving the optimization problem. First, both reservoir level and downstream flow
 396 rates should be within some specified limit. Secondly, maximum flow through the turbine
 397 should not exceed the turbine capacity. Finally, the mean reservoir level at the end of the
 398 simulation should be same as that at the beginning. This ensures that the reservoir is not
 399 emptied at the end of the optimization cycle. The RDO problem reads:

$$\begin{aligned}
 & \arg \min \quad -\beta\mu_R + (1 - \beta)\sigma_R \\
 & \text{s.t.} \quad \mu_{f_t(i)} - 3\sigma_{f_t(i)} \geq 0, \quad \forall i \\
 & \quad \mu_{f_t(i)} + 3\sigma_{f_t(i)} \leq 25000, \quad \forall i \\
 & \quad \mu_{f_t(i)} - 3\sigma_{f_t(i)} + \mu_{f_s(i)} - 3\sigma_{f_s(i)} \geq 500 \quad \forall i \\
 & \quad \left| \left(\mu_{f_t(i)} + 3\sigma_{f_t(i)} + \mu_{f_s(i)} + 3\sigma_{f_s(i)} - \mu_{f_t(i-1)} + 3\sigma_{f_t(i-1)} - \mu_{f_s(i-1)} + 3\sigma_{f_s(i-1)} \right) \right| \leq 500, \quad \forall i \\
 & \quad \mu_{S(i)} - 3\sigma_{S(i)} \geq 50000, \quad \forall i \\
 & \quad \mu_{S(i)} + 3\sigma_{S(i)} \leq 100000, \quad \forall i \\
 & \quad \mu_{S(\text{end})} = 90000
 \end{aligned} \tag{32}$$

400 where $\mu(\bullet)$ and $\sigma(\bullet)$, respectively, denote the mean and standard deviation. β in Eq. (32)
 401 in the weight factor. The objective of this work is to determine f_t and f_s that minimizes
 402 the objective function defined in Eq. (32).

403 7.3. Results and discussion

404 The proposed approaches have been utilized to solve the optimization problem given in
 405 Eq. (32). Since generating benchmark solution using the MCS based DEA requires consider-
 406 able time (approximately 35 days on a system with Xeon processor with 24 cores and 48 Gb
 407 ram), the proposed approach has been validated only at $\beta = 0.5$. Table 9 shows the results
 408 obtained using the proposed approaches. While the high fidelity PCFE based DEA overpre-
 409 dicts the mean revenue at $\beta = 0.5$ by 0.01%, low fidelity PCFE based DEA underpredicts
 410 the same by 2.07%. As for the standard deviation of revenue at $\beta = 0.5$, high fidelity PCFE
 411 based DEA and low fidelity PCFE based DEA underpredicts the result by 3.2% and 6.01%
 412 respectively. As for the computational cost, while high fidelity PCFE based DEA requires
 413 1500 actual simulations, the low fidelity PCFE based DEA requires 1200 actual simulations.
 414 For generating the benchmark solution, 3×10^6 (the solution converges at 200 (objective

415 function call) \times 15000 (number of function call for MCS)) number of actual simulations are
 416 required.

417 One interesting aspect observed in Table 9 is that the flow through spillways are almost zero.
 418 This indicates that the problem in hand can be simplified by setting flow through spillway
 419 to be zero. That way, the reduced problem will have 12 design variables and 36 random
 420 variables. However, this observation may not be true for all hydroelectric dam models and
 421 hence, one must be careful before considering such simplifications.

422 In order to have a better outlook in the problem, the hydroelectric dam optimization has
 423 been carried out corresponding to various values of β . For all the cases, high fidelity PCFE
 424 based DEA has been employed due to its superior performance. Fig. 6 shows the variation
 425 of mean and standard deviation of revenue. As expected, increase in β results in increase
 426 of both mean and standard deviation of revenue. This is logical because of the presence
 427 of negative sign (indicating maximization of the mean revenue) in the objective function
 428 (Eq. (32)). It is further observed that increase in β beyond 0.5 has no effect on the results
 429 (optimum values corresponding to $\beta = 0.5$ and $\beta = 0.6$ are identical). Hence, results beyond
 $\beta = 0.6$ have not been computed.

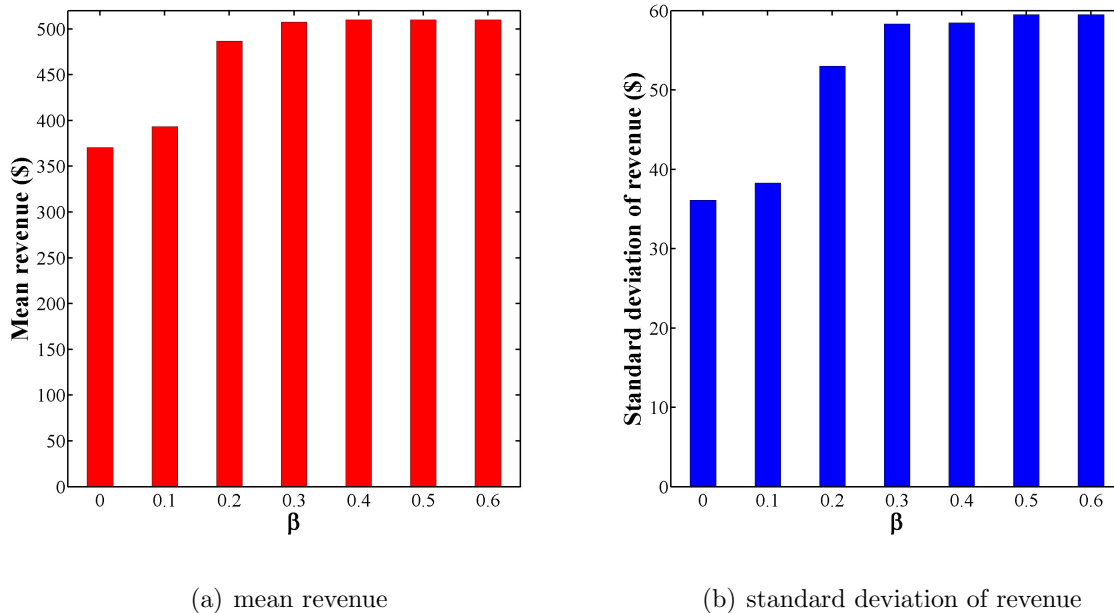


Figure 6: Variation of optimum mean and standard deviation of revenue generated with β .

Table 9: Validation of the proposed approaches for hydroelectric dam optimization

Variable	DEA-MCS	LF DEA-PCFE	HF DEA-PCFE
$f_t(1)$	800	1001.685	800.47
$f_t(2)$	800	802.38	806.1148
$f_t(3)$	800	800.02	800.139
$f_t(4)$	800	800.09	817.10
$f_t(5)$	800	800.85	801.39
$f_t(6)$	800	800.04	800.02
$f_t(7)$	840.69	999.39	878.535
$f_t(8)$	1040.69	967.97	1028.078
$f_t(9)$	1240.69	1167.952	1228.078
$f_t(10)$	1440.69	1367.93	1428.078
$f_t(11)$	1640.69	1567.92	1628.078
$f_t(12)$	1840.69	1767.92	1828.077
$f_s(1)$	2.53×10^{-10}	1.40×10^{-14}	9.88×10^{-8}
$f_s(2)$	1.36×10^{-10}	1.51×10^{-7}	8.43×10^{-8}
$f_s(3)$	7.89×10^{-10}	5.66×10^{-12}	2.87×10^{-7}
$f_s(4)$	4.75×10^{-12}	6.36×10^{-12}	8.88×10^{-20}
$f_s(5)$	2.32×10^{-10}	3.53×10^{-9}	2.61×10^{-7}
$f_s(6)$	1.62×10^{-11}	3.47×10^{-9}	9.75×10^{-14}
$f_s(7)$	2.53×10^{-14}	1.41×10^{-16}	1.44×10^{-20}
$f_s(8)$	1.53×10^{-11}	2.44×10^{-9}	1.92×10^{-19}
$f_s(9)$	1.11×10^{-11}	4.50×10^{-9}	8.86×10^{-19}
$f_s(10)$	1.66×10^{-10}	1.05×10^{-7}	1.93×10^{-8}
$f_s(11)$	3.07×10^{-10}	2.43×10^{-8}	2.44×10^{-9}
$f_s(12)$	3.55×10^{-10}	2.53×10^{-10}	1.36×10^{-8}
μ_R	510.032	499.43	510.088
σ_R	61.48	57.78	59.51

431 8. Conclusion

432 In this work, two novel approaches for robust design optimization (RDO) have been pre-
 433 sented. Both the methods presented utilize polynomial correlated function expansion (PCFE)
 434 to estimate the second moment properties of response and differential evolution algorithm
 435 (DEA) for solving the optimization problem. The first approach, referred to here as low-
 436 fidelity PCFE based DEA, is highly efficient and can be utilized to obtain an initial estimate
 437 for the RDO problems. On contrary, the second approach, referred to here as, high-fidelity
 438 PCFE based DEA, provides an accurate estimate for the RDO problems.

439 The proposed approaches have been utilized for solving three benchmark RDO problems.
 440 Results obtained have been compared with other popular RDO techniques. It is observed
 441 that for both the problems, the proposed approaches outperforms the popular techniques,
 442 both in terms of accuracy and efficiency. Finally, the proposed approach has been utilized
 443 for RDO of a hydroelectric dam, demonstrating its capability in solving large scale problems.

444 Acknowledgement

445 SC and RC acknowledges the support of CSIR via grant no. 22(0712)/16/EMR-II. TC
 446 acknowledges the support of MHRD, Government of India.

447 Appendix A. Formulation of weight matrix

448 The weight matrix (\mathbf{W}) is formulated based on the hierarchical orthogonality of the com-
 449 ponent functions which requires the higher order component function to be orthogonal with
 450 all the lower order component function. Thus, a first-order component function should be
 451 orthogonal to the zeroth-order component function (g_0). The orthogonality between first-
 452 and zeroth-order component function requires

$$\int g_0 \left(\sum_k \alpha_k^{(i)i} \psi_k^i(x_i) \right) \varpi_i dx_i = 0 \quad (\text{A.1})$$

453 where ϖ_i represents the PDF of x_i . Note that g_0 is the mean response and may not be zero.

454 Thus,

$$\int \left(\sum_k \alpha_k^{(i)i} \psi_k^i(x_i) \right) \varpi_i dx_i = 0 \quad (\text{A.2})$$

455 Eq. (A.2) can be represented as

$$\frac{1}{N} \sum_{n=1}^N \sum_k \alpha_k^{(ij)i} \psi_k^i(x_i^n) = 0 \quad (\text{A.3})$$

456 Rewriting Eq. (A.3) in vectorial form

$$\mathbf{G}_1(x_i)^T \boldsymbol{\alpha}_1^i = 0, \quad \forall i \quad (\text{A.4})$$

457 Therefore, the objective function for first-order PCFE is

$$O_1^i = \frac{1}{2} (\boldsymbol{\alpha}_1^i)^T \mathbf{W}_1^i (\boldsymbol{\alpha}_1^i) \quad (\text{A.5})$$

458 where

$$\mathbf{W}_1^i = [\mathbf{G}_1(x_i)] [\mathbf{G}_1(x_i)]^T \quad (\text{A.6})$$

459 Similarly, the second-order component function needs to be orthogonal to both zeroth- and
460 first-order component function. The same can be achieved by setting the second-order com-
461 ponent function orthogonal to all the basis contained in lower order component function.

462 The orthogonality of the second-order component function and g_0 is represented as

$$\int \left(\sum_k \alpha_k^{(ij)i} \psi_k^i(x_i) + \sum_k \alpha_k^{(ij)j} \psi_k^j(x_j) + \sum_l \sum_m \alpha_{lm}^{(ij)ij} \psi_l^i(x_i) \psi_m^j(x_j) \right) \varpi_{ij} dx_i dx_j = 0 \quad (\text{A.7})$$

463 where ϖ_{ij} is the joint PDF of x_i and x_j . Rewriting Eq. (A.7) as

$$\frac{1}{N} \sum_{p=1}^N \left(\sum_k \alpha_k^{(ij)i} \psi_k^i(x_i^p) + \sum_k \alpha_k^{(ij)j} \psi_k^j(x_j^p) + \sum_l \sum_m \alpha_{lm}^{(ij)ij} \psi_l^i(x_i^p) \psi_m^j(x_j^p) \right) = 0 \quad (\text{A.8})$$

464 Writing Eq. (A.8) in vectorial notation

$$[\mathbf{G}_0^{ij}]^T [\boldsymbol{\alpha}_2^{ij}] = 0 \quad (\text{A.9})$$

465 Let us assume $\psi_r^i(x_i)$ to be the basis of first-order component function. Thus, the orthogo-
466 nality between second-order component function and $\psi_r^i(x_i)$ is given as

$$\int \psi_r^i(x_i) \left(\sum_k \alpha_k^{(ij)i} \psi_k^i(x_i) + \sum_k \alpha_k^{(ij)j} \psi_k^j(x_j) + \sum_l \sum_m \alpha_{lm}^{(ij)ij} \psi_l^i(x_i) \psi_m^j(x_j) \right) \varpi_{ij} dx_i dx_j = 0 \quad (\text{A.10})$$

467 Again expressing Eq. (A.10) as a summation series

$$\begin{aligned} & \frac{1}{N} \sum_{p=1}^N \left(\sum_k \alpha_k^{(ij)i} \psi_r^i(x_i^p) \psi_k^i(x_i^p) + \sum_k \alpha_k^{(ij)j} \psi_r^i(x_i^p) \psi_k^j(x_j^p) \right) \\ & + \frac{1}{N} \sum_{p=1}^N \sum_l \sum_m \alpha_{lm}^{(ij)ij} \psi_r^i(x_i^p) \psi_l^i(x_i^p) \psi_m^j(x_j^p) = 0 \end{aligned} \quad (\text{A.11})$$

468 Writing in vectorial notation

$$[\mathbf{G}_{ir}^{ij}]^T [\boldsymbol{\alpha}_2^{ij}] = 0 \quad (\text{A.12})$$

469 Performing similar operation on the basis of component function and second-order compo-
470 nent function

$$[\mathbf{G}_{jr}^{ij}]^T [\boldsymbol{\alpha}_2^{ij}] = 0 \quad (\text{A.13})$$

471 Combining Eq. (A.9), Eq. (A.12) and Eq. (A.13), the objective function for second-order
472 component function is given as

$$\begin{aligned} O_2^{ij} &= \frac{1}{2} [\boldsymbol{\alpha}_2^{ij}]^T [\mathbf{G}_2^{ij}] [\mathbf{G}_2^{ij}]^T [\boldsymbol{\alpha}_2^{ij}] \\ &= \frac{1}{2} [\boldsymbol{\alpha}_2^{ij}]^T [\mathbf{W}_2^{ij}] [\boldsymbol{\alpha}_2^{ij}] \end{aligned} \quad (\text{A.14})$$

473 The combined objective function for second-order PCFE is given as

$$\begin{aligned} O &= \sum_i O_1^i + \sum_{1 \leq i < j \leq N} O_2^{ij} \\ &= \frac{1}{2} \boldsymbol{\alpha}^T \mathbf{W} \boldsymbol{\alpha} \end{aligned} \quad (\text{A.15})$$

474 where

$$\mathbf{W} = \begin{bmatrix} \mathbf{W}_1^1 & 0 & \cdots & 0 & 0 & \cdots & 0 \\ 0 & \mathbf{W}_1^2 & \cdots & 0 & 0 & \cdots & 0 \\ \vdots & \vdots & \ddots & \vdots & \vdots & \ddots & \vdots \\ 0 & 0 & \cdots & \mathbf{W}_1^N & 0 & \cdots & 0 \\ 0 & 0 & \cdots & 0 & \mathbf{W}_2^{12} & \cdots & 0 \\ \vdots & \vdots & \ddots & \vdots & \vdots & \ddots & \vdots \\ 0 & 0 & \cdots & 0 & 0 & \cdots & \mathbf{W}_2^{(N-1)N} \end{bmatrix} \quad (\text{A.16})$$

475

476 **References**

- 477 [1] G. Taguchi, Quality engineering through design optimization, Krauss International Pub-
478 lications, White Plains, NY, 1986.
- 479 [2] J. Marczyk, Stochastic multidisciplinary improvement: Beyond optimization, American
480 Institute of Aeronautics and Astronautics (2000) AIAA-2000-4929.
- 481 [3] J. Fang, Y. Gao, G. Sun, C. Xu, Q. Li, Multiobjective robust design optimization of
482 fatigue life for a truck cab, Reliability Engineering and System Safety 135 (2015) 1–8.
- 483 [4] M. Diez, D. Peri, Robust optimization for ship concept design, Ocean Engineering 37
484 (2010) 966–977.
- 485 [5] B. K. Roy, S. Chakraborty, Robust optimum design of base isolation system in seismic
486 vibration control of structures under random system parameters, Structural Safety 55
487 (2015) 49–59.
- 488 [6] B. K. Roy, S. Chakraborty, S. Mishra, Robust optimum design of base isolation system
489 in seismic vibration control of structures under uncertain bounded system parameters,
490 Journal of Vibration and Control 20 (2014) 786–800.
- 491 [7] M. Xiong, F. C. Arnett, X. Guo, H. Xiong, X. Zhou, Differential dynamic properties of
492 scleroderma fibroblasts in response to perturbation of environmental stimuli, PloS one
493 3 (2) (2008) e1693:1–e1693:12.
- 494 [8] M. Kamiski, Stochastic perturbation approach to the wavelet-based analysis, Numerical
495 Linear Algebra with Applications 11 (4) (2004) 355–370.
- 496 [9] B. Huang, X. Du, Analytical robustness assessment for robust design, Structural and
497 Multidisciplinary Optimization 34 (2) (2007) 123–137.
- 498 [10] R. Rubenstein, Simulation and the Monte Carlo method, Wiley, New York, 1981.
- 499 [11] S. Tamimi, B. Amadei, D. M. Frangopol, Monte-Carlo simulation of rock slope reliabil-
500 ity, Computers & Structures 33 (6) (1989) 1495–1505.

- 501 [12] W. Zhao, J. K. Liu, X. Y. Li, Q. W. Yang, Y. Y. Chen, A moving kriging interpolation
502 response surface method for structural reliability analysis, *CMES-Computer Modeling*
503 *in Engineering & Sciences* 93 (6) (2013) 469–488.
- 504 [13] S. Biswas, S. Chakraborty, S. Chandra, I. Ghosh, Kriging based approach for estimation
505 of vehicular speed and passenger car units on an urban arterial, *Journal of Transporta-*
506 *tion Engineering, Part A: Systems*.
- 507 [14] T. Mukhopadhyay, S. Chakraborty, S. Dey, S. Adhikari, R. Chowdhury, A Critical
508 Assessment of Kriging Model Variants for High-Fidelity Uncertainty Quantification in
509 Dynamics of composite Shells, *Archives of Computational Methods in Engineering* ((Ac-
510 cepted)). doi:10.1007/s11831-016-9178-z.
- 511 [15] B. Echard, N. Gayton, M. Lemaire, N. Relun, A combined importance sampling and
512 kriging reliability method for small failure probabilities with time-demanding numerical
513 models, *Reliability Engineering & System Safety* 111 (2013) 232–240.
- 514 [16] S. H. Ng, J. Yin, Bayesian kriging analysis and design for stochastic simulations, *ACM*
515 *Transactions on Modeling and Computer Simulation* 22 (3) (2012) 17:1–26.
- 516 [17] K.-H. Lee, G.-J. Park, A Global Robust Optimization Using Kriging Based Approxi-
517 mation Model, *JSME International Journal Series C* 49 (3) (2006) 779–788.
- 518 [18] B. Pascual, S. Adhikari, Combined parametric-nonparametric uncertainty quantification
519 using random matrix theory and polynomial chaos expansion, *Computers & Structures*
520 112 (2012) 364–379.
- 521 [19] Pascual, B. and Adhikari, S., A reduced polynomial chaos expansion method for the
522 stochastic finite element analysis, *Sadhana-Academy Proceedings in Engineering Sci-*
523 *ences* 37 (3) (2012) 319–340.
- 524 [20] A. A. Taflanidis, S.-H. Cheung, Stochastic sampling using moving least squares response
525 surface approximations, *Probabilistic Engineering Mechanics* 28 (SI) (2012) 216–224.

- 526 [21] S. Goswami, S. Chakraborty, S. Ghosh, Adaptive response surface method in structural
527 response approximation under uncertainty, in: International Conference on Structural
528 Engineering and Mechanics, 2013, pp. 194–202.
- 529 [22] E. F. Bollig, N. Flyer, G. Erlebacher, Solution to pdes using radial basis function finite-
530 differences (rbf-fd) on multiple gpus, *Journal of Computational Physics* 231 (21) (2012)
531 7133–7151.
- 532 [23] A. A. Jamshidi, M. J. Kirby, Skew-radial basis function expansions for empirical mod-
533 eling, *Siam Journal on Scientific Computing* 31 (6) (2010) 4715–4743.
- 534 [24] S. Marchi, G. Santin, A new stable basis for radial basis function interpolation, *Journal*
535 *of Computational and Applied Mathematics* 253 (2013) 1–13.
- 536 [25] S. Chakraborty, R. Chowdhury, Polynomial Correlated Function Expansion for Non-
537 linear Stochastic Dynamic Analysis, *Journal of Engineering Mechanics* 141 (3) (2014)
538 04014132:1—04014132:11.
- 539 [26] S. Chakraborty, R. Chowdhury, A semi-analytical framework for structural reliability
540 analysis, *Computer Methods in Applied Mechanics and Engineering* 289 (1) (2015) 475–
541 497.
- 542 [27] S. Chakraborty, R. Chowdhury, Assessment of polynomial correlated function expansion
543 for high-fidelity structural reliability analysis, *Structural Safety* 59 (2016) 9–19.
- 544 [28] S. Chakraborty, B. Mandal, R. Chowdhury, A. Chakrabarti, Stochastic free vibration
545 analysis of laminated composite plates using polynomial correlated function expansion,
546 *Composite Structures* 135 (2016) 236–249.
- 547 [29] S. Chakraborty, R. Chowdhury, Sequential experimental design based generalised
548 ANOVA, *Journal of Computational Physics* 317 (2016) 15–32.
- 549 [30] S. Chakraborty, R. Chowdhury, Modelling uncertainty in incompressible flow simula-
550 tion using Galerkin based generalized ANOVA, *Computer Physics Communications* 208
551 (2016) 73–91.

- 552 [31] S. Chakraborty, R. Chowdhury, A hybrid approach for global sensitivity analysis, Reli-
553 ability Engineering & System Safety doi:10.1016/j.res.2016.10.013.
- 554 [32] L. T. Stutz, R. A. Tenenbaum, R. A. P. Correa, The differential evolution method
555 applied to continuum damage identification via flexibility matrix, Journal of sound and
556 vibration 345 (2015) 86–102.
- 557 [33] R. Storn, K. Price, Differential evolution - a simple and efficient heuristic for global
558 optimization over continuous spaces, Journal of Global Optimization 11 (1997) 341–
559 359.
- 560 [34] S. Biswas, S. Kundu, S. Das, Inducing niching behavior in differential evolution through
561 local information sharing, Evolutionary Computation, IEEE Transactions on 19 (2)
562 (2015) 246–263.
- 563 [35] S. Das, P. Suganthan, Differential evolution: A survey of the state-of-the-art, Evolu-
564 tionary Computation, IEEE Transactions on 15 (1) (2011) 4–31.
- 565 [36] C. Zang, M. I. Friswell, J. E. Mottershead, A review of robust optimal design and its
566 application in dynamics, Computer & Structures 83 (2005) 315–326.
- 567 [37] H. G. Beyer, B. Sendhoff, Robust optimization – a comprehensive survey, Computer
568 Methods in Applied Mechanics and Engineering 196 (2007) 3190–3218.
- 569 [38] G. Hooker, Generalized Functional ANOVA Diagnostics for High-Dimensional Functions
570 of Dependent Variables, Journal of Computational and Graphical Statistics 16 (3) (2007)
571 709–732.
- 572 [39] G. Li, H. Rabitz, General formulation of HDMR component functions with independent
573 and correlated variables, Journal of Mathematical Chemistry 50 (1) (2012) 99–130.
- 574 [40] S. Chakraborty, R. Chowdhury, Multivariate function approximations using D-MORPH
575 algorithm, Applied Mathematical Modelling 39 (2015) 7155–7180.
- 576 [41] V. J. Beltrani, Exploring quantum control landscapes, Ph.D. thesis, Princeton Univer-
577 sity, Princeton, NJ 08544, United States (2012).

- 578 [42] G. Li, H. Rabitz, D-MORPH regression: application to modeling with unknown param-
579 eters more than observation data, *Journal of Mathematical Chemistry* 48 (4) (2010)
580 1010–1035.
- 581 [43] G. Li, R. Rey-de Castro, H. Rabitz, D-MORPH regression for modeling with fewer
582 unknown parameters than observation data, *Journal of Mathematical Chemistry* 50 (7)
583 (2012) 1747–1764.
- 584 [44] C. R. Rao, S. K. Mitra, Generalized inverse of a matrix and its applications, in: *Pro-*
585 *ceedings of the Sixth Berkeley Symposium on Mathematical Statistics and Probability,*
586 1971.
- 587 [45] P. Bratley, B. L. Fox, Implementing Sobols quasirandom sequence generator, *ACM*
588 *Transactions on Mathematical Software* 14 (1) (1988) 88–100.
- 589 [46] I. M. Sobol, Uniformly distributed sequences with an additional uniform property, *USSR*
590 *Computational Mathematics and Mathematical Physics* 16 (1976) 236–242.
- 591 [47] S. Lee, W. Chen, B. Kwak, Robust design with arbitrary distributions using gauss-
592 type quadrature formula, *Structural and Multidisciplinary Optimization* 39 (3) (2009)
593 227–243.
- 594 [48] I. Doltsinis, Z. Kang, Robust design of structures using optimization methods, *Computer*
595 *Methods in Applied Mechanics and Engineering* 193 (23-26) (2004) 2221–2237.
- 596 [49] E. Patelli, M. Broggi, M. de Angelis, M. Beer, OpenCossan: An Efficient Open Tool for
597 Dealing with Epistemic and Aleatory Uncertainties, in: *Vulnerability, Uncertainty, and*
598 *Risk,* American Society of Civil Engineers, Reston, VA, 2014, pp. 2564–2573.
- 599 [50] R. d. S. Motta, S. M. B. Afonso, P. R. Lyra, R. B. Willmersdorf, Development of a com-
600 putational efficient tool for robust structural optimization, *Engineering Computations*
601 32 (2) (2015) 258–288.
- 602 [51] R. IEEE, Dynamic Models for Steam and Hydro Turbines in Power System Studies,
603 *IEEE Transactions on Power Apparatus and Systems* PAS-92 (6) (1973) 1904–1915.

- 604 [52] W. group IEEE, Hydraulic turbine and turbine control models for system dynamic
605 studies, IEEE Transactions on Power Systems 7 (1) (1992) 167–179.
- 606 [53] S. DeLand, Solving large-scale optimization problems with MATLAB: A hydroelectric
607 flow example (2012).

ACCEPTED MANUSCRIPT